

An Empirical Study on Corner Detection to Extract Buildings in Very High Resolution Satellite Images

Leyden Martinez-Fonte, Sidharta Gautama and Wilfried Philips
Department of Telecommunications and Information Processing, Ghent University
Sint-Pietersnieuwstraat 41, B-9000 Ghent, Belgium
Phone: +32 (0)9 264 3412 Fax: +32 (0)9 264 4295
E-mail: lmartine@telin.Ugent.be

Abstract—In this paper, we examine the detection of man-made structures in Very High Resolution (VHR) satellite images. The first step of this detection consists of describing the objects' geometry through corners. Not only are corners an important cue for the presence of geometric primitives. They are also essential in forming higher-level shapes like rectangles and polygons through perceptual grouping techniques. In this paper, we examine several corner detectors and compare their performance in terms of detection rate, whereby the corners of interest are those defined by man-made objects. The detectors studied are a gradient-based method based on the Harris detector and the SUSAN detector. Results were analyzed through ROC curves.

Keywords— corner; VHS satellite images; Harris; SUSAN; ROC curves analysis.

I. INTRODUCTION

Up till now, a standard method to extract objects is through spectral classification or segmentation. In contrast, we focus on the geometric content of the image in terms of lines, corners, rectangles, etc. The idea is based on the hypothesis that man-made objects, like buildings, often appear as regular geometric structures. Describing the information content in terms of these primitives should allow for a better differentiation between real man-made structures and other types of land covers.

The first step of our research deals with the possibility of describing the geometrical contents of man-made objects (specifically buildings) present in VHS panchromatic satellite images [1], by using *basic* corner detectors only.

By *basic* we imply that no other features (like edges or texture, for instance) are taken into account in the analysis, and only a local analysis is performed.

Corners are the features chosen to describe the geometrical contents. By *corners* we mean 2D features like L-corners and T-, Y-, X-junctions. In any image there are fewer corners than edge features, and yet they hold the information regarding geometry of man-made objects, characterized by a regular structure.

The objective of this paper was to determine how accurate the results of this approach can be, and whether if other stages are needed to get the information.

II. MATERIALS AND METHODS

A. Very High Resolution Satellite Images

These images have a spatial resolution of 1 meter in their panchromatic version. Specifically, our images come from IKONOS and Quickbird satellites.

B. Selection of Corner Detectors

Among the most cited corner detectors in the literature [2-12] we find the Harris detector [13] and SUSAN [14]. So, we choose them for this evaluation. In the case of the Harris detector, for our analysis an improved version developed by Noble [15] is used.

One reason for including SUSAN in our study was that we wanted to see if this method could detect rounded corners, which are difficult to find with gradient-based methods, like the Harris detector.

C. The Harris Corner Detector

This method is based on the assumption that corners are associated with maxima of the local autocorrelation function. It calculates a "cornerness" value C for each pixel of the image, and if C is a local maximum above certain threshold, the pixel is declared a corner.

In practice, the cornerness is calculated through the directional derivatives of the intensities (I_x , I_y , I_{xy}), resulting in equations 1 and 2. Derivatives are

determined by convolving the image by a kernel of the correspondent derivative of a Gaussian, and k is a constant with a generally assumed value of 0.04 [10].

$$M = \begin{bmatrix} (I_x)^2 & I_{xy} \\ I_{yx} & (I_y)^2 \end{bmatrix} \quad (1)$$

$$C = \det(M) - k \operatorname{Tr}(M) \quad (2)$$

Equation 3 is the variation proposed by Noble [14]. It improves the results of the Harris detector, and in some papers it is directly referred to as Harris detector [10].

$$C = \frac{\det(M)}{\operatorname{Tr}(M) + \varepsilon} \quad (3)$$

In both Harris detector and its variation by Noble, a local maxima search is performed as a final step of the algorithm.

D. The SUSAN Corner Detector

This detector does not use spatial derivatives nor smoothes the image. Instead, a circular mask is applied around every pixel, and the greyscale values of all the pixels within the mask are compared to that of the center pixel (the “nucleus”). All pixels with similar brightness to that of the nucleus are assumed to be part of the *Univalue Segment Assimilating Nucleus*: USAN.

Figure 1 shows the masks with pixels with similar brightness to the nucleus in black (USAN), and the pixels with different brightness colored in white. The authors of the method consider a pixel as a corner (case **a** in Figure 1) when its USAN area is less than half the total mask area. The exact position of the corner will be indicated by the local minimum in USAN area.

The circular mask includes 37 pixels symmetrically distributed around its center. Every pixel can add up to 100 units to the USAN, according to the formula:

$$c(r, r_0) = 100 \exp \left(- \left(\frac{I(r) - I(r_0)}{t} \right)^6 \right) \quad (4)$$

where r_0 is the nucleus, r is any other point of the mask, $I(r)$ is the brightness of any pixel, and t is the “brightness-difference” threshold.

E. Modifications to Standard SUSAN

We wanted to investigate the effects on our results of modifying several parts of this algorithm. Each of these variations was implemented separately.

The aspects changed were:

- **Size of the mask:** *a.* 25 pixels, *b.* 37 pixels (standard), *c.* 49 pixels, *d.* 119 pixels.

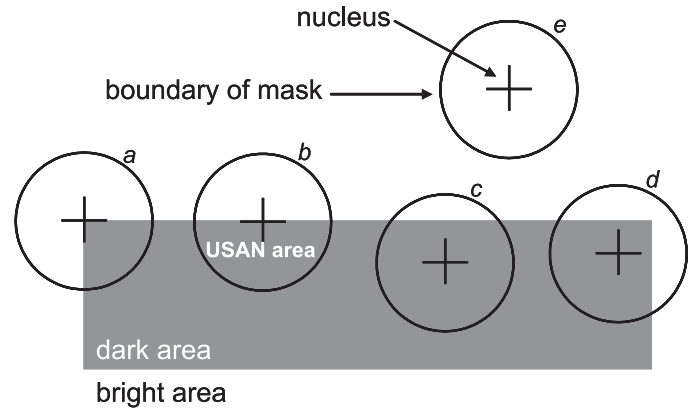


Figure 1. The principle behind SUSAN.

- **Brightness-difference threshold:** fixed threshold for the whole image (standard), adaptive threshold.
- **Brightness-difference equation:** binary, exponential (standard).

In SUSAN the contribution of every pixel to the USAN is an exponential function of its brightness-difference with the nucleus (4). A binary approach (5) was also discussed by the authors of SUSAN, but the exponential contribution was the one included in the final method. In this study we will compare the binary approach as well.

$$c(r, r_0) = \begin{cases} c = 100 & |I(r) - I(r_0)| \leq t \\ c = 0 & |I(r) - I(r_0)| > t \end{cases} \quad (5)$$

- **Search for local maxima:** *a.* fixed size for search-area (standard); *b.* variable area size for search-area: 3x3, 7x7, 5x5, 9x9; *c.* skip the search of local maxima.

F. Relevant Corners for our Application

The ground truth (GT) of this study consists of annotated image extracts containing relevant types of man-made structures, in which the pertinent corners have been identified. This GT allows us to define the optimal detection rate and the associated parameter set through the analysis of ROC curves.

We consider as Relevant Corners (GT corners): corners of objects (man-made or not) with a regular structure (like polygons), corners of the shadows of the previous objects.

The following cases are treated as False Alarms: features located on edges; features belonging to: natural objects (like forest), objects whose border length is smaller than 2 pixels (like lines), rounded objects, shadows caused by these objects; features caused by noise.

In any of the previous cases, if the length of the border is between 3 and 4 pixels, we ignore the detection there.

G. Analysis Methodology

To analyze the results, and to compare the detectors, ROC curves were generated following the methodology proposed by Bowyer et al. [16]:

1. For a detector, a set of values is generated uniformly covering its parameters' range. If the detector has P parameters, four uniformly distributed values are calculated for each parameter. The combination of the four values of each of the P parameters will give 4^P points in the detector's parameter space.
2. Each image is analyzed with the detector for the 4^P parameters points. The detected feature map is compared to the GT, resulting in a count of undetected GT corners (UGT) and false alarms (FA).
3. Each pair (UGT,FA) plots a point in the ROC space. However, only those points closer to the origin (where both UGT and FA are zero), will be included in the ROC curve.
4. Next, refinement in the sampling of each parameter is considered. The number of values taken into account per parameter is increased. For instance: if the detector has 2 parameters, then the initial sampling is 4×4 , and the second and third samplings are 7×4 and 4×7 . Steps 2 and 3 are redone for the new samplings and the one with best ROC curve is kept. This adaptive refinement continues for at least two iterations, until the improvement in the ROC curve falls below 5% of the area under the curve.

Bowyer's methodology [16] was originally designed for edge detectors, and the false alarms rate is determined by:

$$\text{False Alarms Rate} = \frac{\text{Number of False Features}}{\text{Total of Pixels of the image}} \quad (5)$$

In any image, the number of corner-features is much lower than the number of edge-features. Consequently, the numbers obtained in (5) are very small, but this does not mean the performance of corner detectors is better than edge detectors. Then, it would be important to be aware that in the images included in this study: 0.01% FA rate is equivalent to 600-900 false alarms, whereas 0.01% UGT would be around 1-3 corners.

Once our images were analyzed with Noble and SUSAN, modifications were added to the latter to see if improvements could be reached on the results. Their results were also included in the ROC curves analysis.

H. Images Used in the Study

A large panchromatic IKONOS image of the city of Ghent was used in this study. From it, several smaller



Figure 2. Sample images that illustrate our analysis.

images were cut. In this paper, two representative images are used: *factory* and *suburbs* (Figure 2). The actual sizes of the images are 283×334 pixels and 244×252 pixels, respectively.

III. RESULTS AND DISCUSSION

A. Standard Noble and SUSAN

Comparing the results of standard Noble and SUSAN (Figure 3), we could appreciate that Noble detects more GT corners than SUSAN. In *suburbs* both methods detect fewer GT corners, and more false alarms appear.

In every case the level of false alarms was high. For instance, in *factory* the lower amount of false alarms signaled by Noble was 54 (0.0005%), and in that same detection only 13 GT corners were detected.

B. Modifications to Standard SUSAN

When the size of the mask decreases, fewer GT corners are found. When it increases, results improve (Figure 5). However, further increases in the mask size do not improve the detection, showing there are limits in the information we can get using only local data.

A very small improvement of the detection of ground truth corners was obtained by using a binary brightness-difference equation (Figure 4). Probably because with the binary approach corners between non-uniformly flat areas could get a higher USAN, and surpass the brightness-difference threshold.

With the adaptive threshold, results were a bit worse than with a fixed threshold for the whole image (Figure 4). In another attempt to improve SUSAN by adapting the threshold [17], only modest improvements were achieved. That attempt focused on a combined edge and corner detection, and in such cases a thinning step can be applied enhance the detection (removing false alarms and recovering missed features). In the case of corners, features are not connected, and a thinning-like process would only be possible using edges information, for instance.

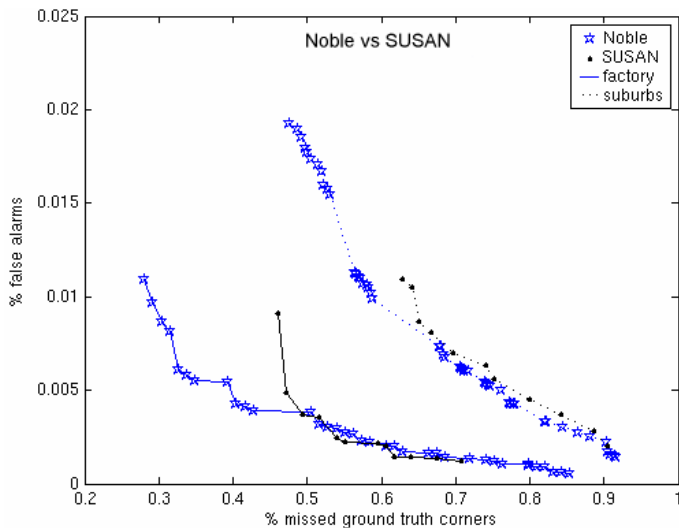


Figure 3. ROC curves for Noble and SUSAN in our images.

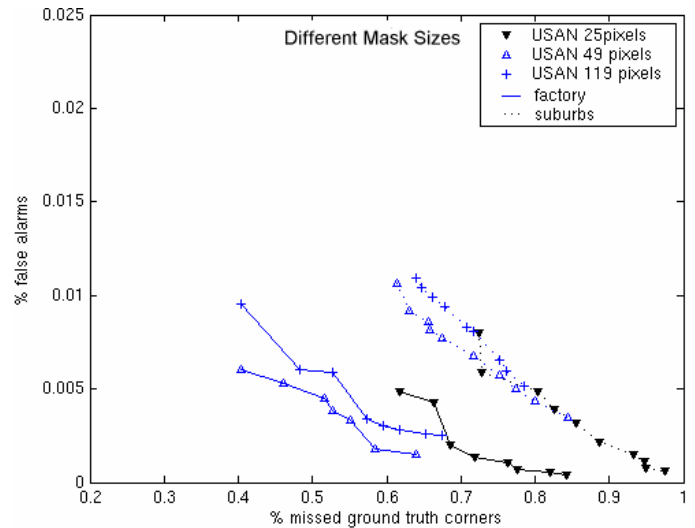


Figure 5. Effect of using different mask sizes.

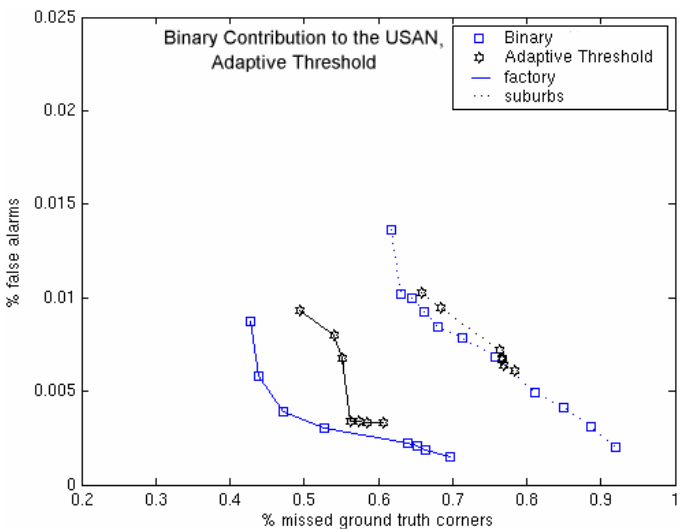


Figure 4. Binary contribution to the USAN, adaptive threshold ROC curves.

The largest number of GT corners were kept using smaller areas to search for local maxima, or by not using this step at all (Figure 6). This shows that many GT corners are removed by this last step of SUSAN, which keeps only the local maxima and removes the other corners. In our images the size and distance between objects is small, so this step has an important influence on the number of ground truth corners that survive at the end of the process. Unfortunately, these SUSAN variants had a much higher false alarm rate than Noble. So, other ways must be found to circumvent the misdetection of the relevant corners.

C. General Results

Missed GT Corners

No method detects every ground truth corner. Some corners are missed by Noble and also by SUSAN (Figure 7). These features often have very low contrast,

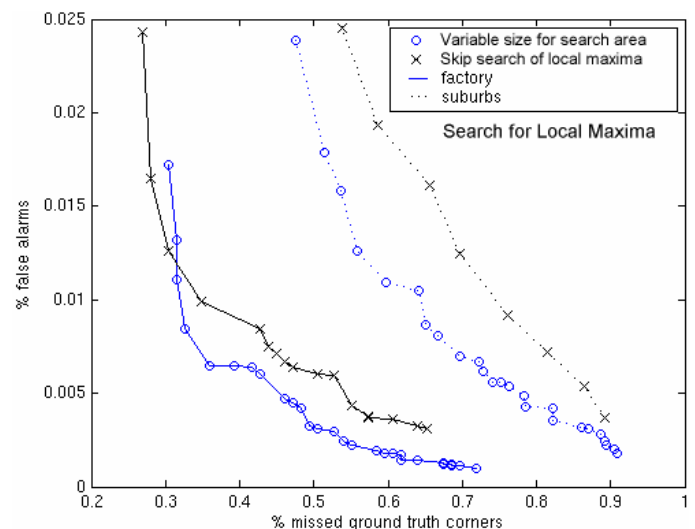


Figure 6. Variations in the search for local maxima in SUSAN.

sometimes the edges that shape them have discontinuities in the surroundings of the corner (due to blurring, shadows or the superposition of two objects). This situation is particularly abundant in *suburbs*, where also objects are small. Extra information would be needed to find these non-locally obvious corners, like following the edges that shape them.

The corners missed only by Noble don't show high values in the gradient nor curvature maps. The corners missed only by SUSAN are between non-uniformly flat areas, which are typical in agriculture fields and in roofs slopes. The latter case corresponds to gradient color areas, whose detection in the artificial image provided by its creators [14] is reached only with a low brightness threshold (which in real cases increases the false alarms). In a real scene like ours, the presence of noise or the fact that roof surfaces are not perfect, makes it more difficult to detect these corners.



Figure 7. GT corners missed by Noble and by SUSAN.

	<i>factory</i>	<i>suburbs</i>
Noble	70%	32%
SUSAN	58%	30%

Table 1. Rate of GT corners detected in the optimum cases.

Table 1 shows the GT corners detection rate for the optimum cases. The false alarms rate can be visually appreciated in Figure 8 for *factory*.

False Alarms

Figure 9 shows the false alarms signaled by all the combinations of the parameter's values. Both methods have numerous texture corners, in forest areas for instance. False corners in Noble appear closer to objects. On the contrary, in SUSAN many false alarms are signaled in almost flat areas and along edges. The fact that SUSAN mistakes many edge-like features as corners has been reported by several researchers who have used it in their work, but it didn't seem to be so important within other applications (e.g. tracking).

IV. CONCLUSIONS

Analyzing the results obtained with a view on the man-made objects recognition goal, we are able to conclude that the sole use of basic corner detector is not enough. In contrast with tracking and matching between images, for instance, where the "kind" of corner is not as important as its permanency or its invariance to rotation; our application is very sensitive to non-relevant features, such as edge-like and texture corners.

On the other hand, it is very important to detect all the relevant corners, because missing one would imply the

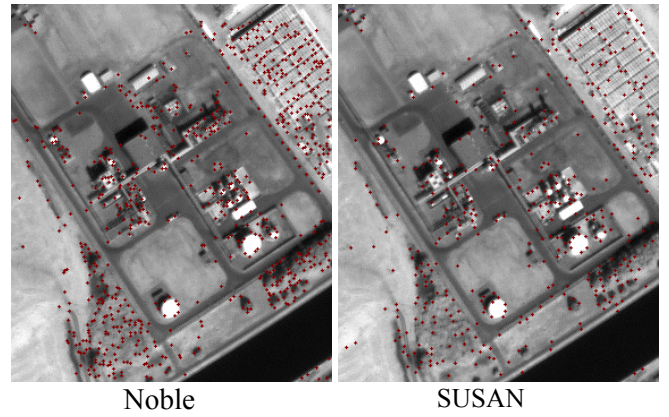


Figure 8. False alarms in the optimal detections in *factory*.

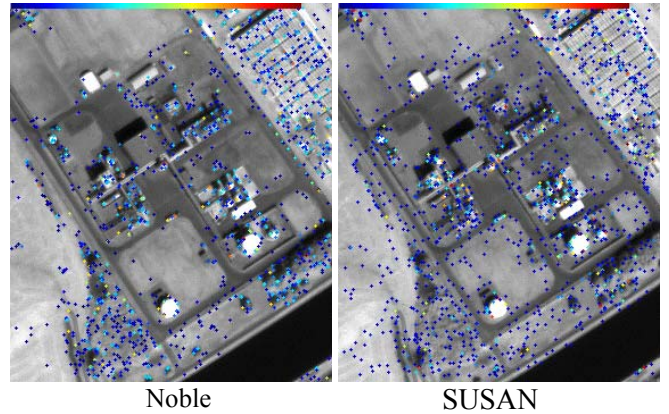


Figure 9. Total of false alarms found in *factory*.

further misdetection of the geometrical shape of at least one object. This couldn't be accomplished with any of the variants studied here, because no method could reach a zero rate of unmatched ground truth.

V. FUTURE WORK

In order to achieve a reliable description of the geometrical contents of the man-made objects in VHS satellite images through corners, further processing involving more than just local information has to be taken into account. Feature detectors are evolving in that direction [5, 18-23], and our application would need to make use of those approaches as well. We have already started preliminary tests with some of them, and further research on this path would be the next step of our investigation. Other directions could be: extending the detection to multispectral analysis, including previous knowledge of the image (like maps information), elimination of shadows, among others.

VI. ACKNOWLEDGEMENTS

We thank Kevin Bowyer and Ping Yan, from University of Notre Dame, for providing us with the source code of the framework to generate ROC curves of edge detectors.

REFERENCES

- [1] TM. Lillesand, RW. Kiefer, Remote Sensing and Image Interpretation, 4th ed., John Wiley & Sons, US, 2000.
- [2] C. Schmid, R. Mohr, C. Bauckhage, Evaluation of Interest Point Detectors, *Int. J. of Computer Vision*, 37(2): 151-172, 2000.
- [3] I. Golightly, D. Jones, Corner Detection and Matching for Visual Tracking During Power Line Inspection, *Image and Vision Computing*, 21: 827-840, 2003.
- [4] Z. Zivkovic, F. van der Heijden, Improving the selection of Feature Points for Tracking, *Pattern Analysis and Applications*, 7(2): 144-150, 2004.
- [5] M. Cazorla, F. Escolano, D. Gallardo, R. Rizo, Junction Detection and Grouping with Probabilistic Edge Models and Bayesian A*, *Pattern Recognition* 35: 1869-1881, 2002.
- [6] P. Skocir, B. Marusic, T. Jurij, A 3D Extension of the SUSAN Filter for Wavelet Video Coding Artifact Removal, *Proceedings of 11th Mediterranean Electrotechnical Conference*, 1:395-398, Cairo, Egypt, 2002.
- [7] SM. Charlwood, PB. James-Roxby, RL. Walke, Adaptive 2-D Feature Detection using Dynamic Reconfiguration, *Proceedings of SPIE-1999 Reconfigurable Technology*, 3844: 141-152, Boston, US, 1999.
- [8] SC. Bae, IS. Kweon, CD. Yoo, COP: a New Corner Detector, *Pattern Recognition Letters*, 23: 1349-1360, 2002.
- [9] RM. Guest, MC. Fairhurst, A Clustering Approach to Corner Point Analysis in Hand Drawn Images, *Proceedings of 16th Int. Conf. on Pattern Recognition*, 13: 940-943, Quebec, Canada, 2002.
- [10] P.I. Rockett, Performance Assessment of Feature Detection Algorithms: a Methodology and Case Study on Corner Detectors, *IEEE Trans. Image Processing*, 12(12): 1668-1676, 2003.
- [11] P. Tissainayagam, D. Suter, Assessing the Performance of Corner Detectors for Point Feature Tracking Applications, *Image and Vision Computing*, 22: 663-679, 2004.
- [12] F. Mohanna, F. Mokhtarian, Performance Evaluation of Corner Detection Algorithms under Similarity and Affine Transforms, *Proceedings of British Machine Vision Conference*, Manchester, UK, 2001.
- [13] C. Harris and M. Stephens, A Combined Corner and Edge Detector, *Proc. 4th Alvey Vision Conference*, Manchester, pp. 147-151, 1988.
- [14] S. M. Smith and J. M. Brady, SUSAN - A New Approach to Low Level Image Processing, *International Journal of Computer Vision*, 23(1): 45-78, 1997.
- [15] A. Noble, Finding Corners, *Image and Vision Computing Journal*, 6(2): 121-128, 1988.
- [16] K. Bowyer, C. Kranenburg and S. Dougherty, Edge Detector Evaluation Using Empirical ROC Curves, *Computer Vision and Image Understanding* 84: 77-103, 2001.
- [17] MM. Pérez, TJ. Dennis, Adaptive Implementation of the SUSAN Method for Image Edge and Feature Detection, *IEEE Int. Conf. on Image Processing*, 2: 394-397, 1997.
- [18] M. Ruzon, C. Tomasi, Edge, Junction, and Corner Detection Using Color Distributions, *IEEE Trans. Patterns Analysis and Machine Intelligence*, 23(11): 1281-1295, 2001.
- [19] M. Idrissa, V. Lacroix, A. Hincq, H. Bruynseels, O. Swartenbroekx, SPOT5 Images for Urbanization Detection, *Proceedings of Advanced Concepts for Intelligent Vision Systems*, Brussels, Belgium, 2004.
- [20] T. Hansen, H. Neumann, Neural Mechanisms for the Robust Representation of Junctions, *Neural Computation* 16: 1013-1037, 2004.
- [21] DR. Martin, CC. Fowlkes, J. Malik, Learning to Detect Natural Image Boundaries Using Local Brightness, Color, and Texture Cues, *IEEE Trans. Pattern Analysis and Machine Intelligence*, 26(5): 530-549, 2004.
- [22] RP. Wurtz, T. Lourens, Extraction and Matching of Symbolic Contour Graphs, *Int. J. Pattern Recognition and Artificial Intel.*, 17(7): 1279-1302, 2003.
- [23] C. Nardinocchi, M. Scaioni, G. Forlani, Building Extraction from LIDAR Data, *Proceedings of IEEE/ISPR Joint Workshop on Remote Sensing and Data Fusion over Urban Areas*, Rome, Italy, 2001.